

# Low-Temperature Annealing Spectrum of Electron-Irradiated Gold and Cadmium\*

WALTER BAUER,<sup>†</sup> JOHN W. DEFORD,<sup>‡</sup> AND JAMES S. KOEHLER  
*Department of Physics, University of Illinois, Urbana, Illinois*

AND

JOHN W. KAUFFMAN  
*Materials Science Department, Northwestern University, Evanston, Illinois*  
 (Received July 2, 1962)

Cadmium and gold of 99.999% purity were irradiated to an integrated flux of  $7.5 \times 10^{17}$  electrons/cm<sup>2</sup> using 3-MeV electrons. The resistivity increase was  $8.5 \times 10^{-9}$   $\Omega$ -cm in gold and  $2.32 \times 10^{-8}$   $\Omega$ -cm in cadmium. The resistivity versus integrated flux curve is linear. Isothermal annealing measurements were made in the region from 8 to 51°K. The resistivity annealing spectrum of gold was derived directly from the isothermal annealing curves. The spectrum consists of at least nine peaks, with 22% of the damage annealing out up to 51°K. These results confirm earlier suggestions that the radiation damage in gold is basically different from that of copper and silver. It is thought that the interstitial in gold differs from that in copper and silver. In connection with the amount of low-temperature annealing, it is thought that focusing and interstitial clustering are important. Deviations from Matthiessen's rule for gold and cadmium are in qualitative agreement with theory. Only qualitative agreement with an earlier experiment on the annealing of cadmium can be confirmed.

## I. INTRODUCTION

IN this experiment, the use of radiation damage in the study of point defects in metals is applied to gold and cadmium. Experiments by Cooper<sup>1</sup> and Herschbach<sup>2</sup> with deuterons, by Ward and Kauffman<sup>3</sup> with electrons, and by Blewitt<sup>4</sup> with neutrons, indicated differences in the stage I annealing of gold and copper. The technique of isothermal annealing and a damage of  $8.5 \times 10^{-9}$   $\Omega$ -cm afforded a greater resolution of the activation energy spectrum than that obtained in reference 3. Basic differences in the annealing of stage I in gold and copper are confirmed.

This paper is divided into four parts. Under the heading of Experimental Procedure the cryostat, specimen preparation, electrical and temperature measurements, and the irradiation are discussed. In the next section, under Data, the method of reduction of the direct experimental values into the graphical results is given. Under Calculations a brief sketch of the mathematical analysis for the computation of the activation energy spectrum is given, and the deviations from Matthiessen's rule in gold and cadmium are discussed. Under Discussion a detailed comparison is made between the annealing spectrum of gold obtained in this experiment and that obtained in the above references.

## II. EXPERIMENTAL PROCEDURE

### Cryostat

The cryostat used in this experiment is the same as the one described by Magnuson, Palmer, and Koehler.<sup>5</sup> The following modifications were made. To reduce the heat input from conduction, the 4-mil copper electrical lead in wires were first brought to liquid-nitrogen temperature by making good contact with the upper part of the liquid-nitrogen shield of the cryostat. The wires were then loosely wrapped several times around the outside of the heat switch and were in poor thermal contact with it. This results in a small temperature gradient in the wires between helium and nitrogen temperatures. Before being attached to the specimens and temperature measuring devices the wires were firmly fastened to the block with a mixture of G.E. varnish 701, toluene, and ethyl alcohol. To reduce the heat input due to radiation, the openings in both the helium and nitrogen shields were covered with 1/2-mil aluminum foil. 1/2- $\times$ 3/8-in. openings on the beam side of the shields and larger openings on the exit side were made to allow the beam to pass through without scattering. Convection heat losses were considered to be minor since the vacuum before irradiation was  $7 \times 10^{-7}$  mm of mercury and changed only slightly during irradiation. With these modifications block temperatures of 5.5 and 7.5°K and liquid helium loss rates of 0.08 liter/h and 0.25 liter/h, respectively, were achieved before and during irradiation.

### Specimen Preparation and Mounting

The cadmium used in this experiment had a nominal purity of 99.999% and was in the form of small chunks. A 6-mm i.d. Pyrex tube coated on the inside with

\* Research supported by the U. S. Atomic Energy Commission.

<sup>†</sup> Based on a thesis submitted in partial fulfillment of the requirements for the degree of Doctor of Philosophy at the University of Illinois. Present address: Atomics International, Canoga Park, California.

<sup>‡</sup> Present address: Department of Physics, University of Utah, Salt Lake City, Utah.

<sup>1</sup> H. G. Cooper, J. S. Koehler, and J. W. Marx, *Phys. Rev.* **97**, 599 (1955).

<sup>2</sup> K. Herschbach, *Phys. Rev.* (to be published).

<sup>3</sup> J. B. Ward and J. W. Kauffman, *Phys. Rev.* **123**, 90 (1961).

<sup>4</sup> T. H. Blewitt, Oak Ridge National Laboratory Report ORNL-3017 (unpublished), p. 30.

<sup>5</sup> G. D. Magnuson, W. Palmer, and J. S. Koehler, *Phys. Rev.* **109**, 1990 (1958).

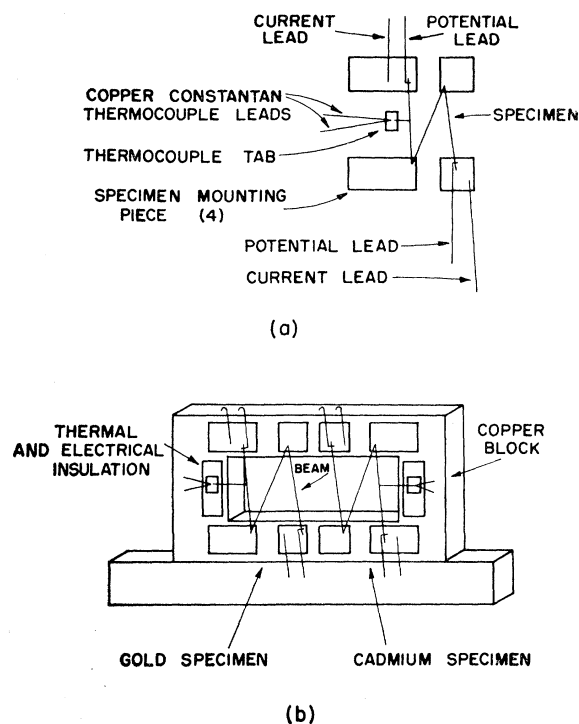


FIG. 1. (a) Specimen and electrical connections. (b) Specimen mounting position on block.

Aquadag and outgassed at 450°C was used to melt several of these chunks into a 150-mil-diam rod. The cadmium was held at 420°C at a pressure of 10 mm of neon for 1 h; then the oven was removed and the glass tube was dropped into cold water. This type of solidification results in many grain boundaries and small average crystal size, which greatly facilitates subsequent cold work. The cadmium rod was then cold rolled to a thickness of 2 mils from which a 5-mil-wide strip was cut with a special foil cutter prepared from tool steel. The authors are indebted to F. Witt for the design of this cutter. From this 2×5 mil rectangular wire a continuous specimen of approximately 3-cm length in the form of a flat zig-zag was prepared. The ends of the specimen were spotwelded to a small piece of 2-mil-thick cadmium on which copper current and potential leads were spotwelded. The corners of the cadmium specimen were also spotwelded to pieces of cadmium. At the center of one side of the specimen a 3-mm long piece of cadmium was spotwelded for the thermocouple attachment, Fig. 1(a). The specimen was then annealed in vacuum at 200°C for 12 h.

The gold was in the form of 2-mil-diam wire of 99.999% purity obtained from the Sigmund Cohn Corporation. A specimen identical in shape to the above was constructed. Pieces of 15-mil gold wire were spotwelded to the flat gold pieces to form a rigid frame. This frame reduced the cold work after the anneal and during the mounting. Gold wires were used for current and

potential leads to eliminate contamination during the anneal. The gold specimen was annealed for 20 h at 600°C in an atmosphere of argon. The gold was cleaned and etched both before spotwelding and before annealing.

The specimens were mounted as shown in Fig. 1(b), electrically insulated from, but in good thermal contact with, the block. This was achieved by applying a thin layer of the above-mentioned G.E. varnish mixture to the block, a strip of Mylar foil, another layer of varnish, and then pressing down the sheets of gold and cadmium to which the specimens were attached. The temperature difference between specimen and block was about 0.1 deg. After the varnish had dried the 15-mil gold frame was cut away without disturbing the specimen.

The  $R_0^\circ\text{C}/R_{4.2^\circ\text{K}}$  ratio of the gold wire used was 1120. The ratio of the mounted specimen made from this wire was 750. The authors attribute the additional residual resistivity to unavoidable cold work during mounting, since resistance measurements after reannealing yielded the original 1120 ratio. The  $R_0^\circ\text{C}/R_{4.2^\circ\text{K}}$  ratio of the mounted cadmium specimen was 1300. No low-temperature strains were detected by residual resistance measurements at 6°K after repeated cycling from room temperature.

### Temperature Measurement

The method used for temperature measurement and control in this experiment was basically the same as that used by Palmer, Magnuson, and Koehler.<sup>5</sup> In the measurement of temperature, a platinum resistance thermometer calibrated by the National Bureau of Standards was used to measure the temperature of the mounting block and a copper constantan difference thermocouple to measure the difference in temperature between specimen and block, Figs. 2(b) and 2(c).

Considerable difficulties were encountered in the use of the thermocouple. The thermoelectric power was known, having been measured by Magnuson *et al.*<sup>5</sup> For the operating conditions, readings of the order of 1  $\mu\text{V}$  were to be expected and thus parasitic emf's in the copper lead wires, or rather their reproducibility, posed severe problems. It was found that relatively small changes in the surroundings could cause the value of the parasitic emf's at a given temperature to change by several tenths of a microvolt. By careful control of the surroundings, it was ultimately possible to make the parasitic emf's reproducible to within 0.05  $\mu\text{V}$ . For comparison, values of the thermoelectric power in this range are: 3.5  $\mu\text{V}/\text{deg}$  at 10°K, 5.2 at 20°K, 10.3 at 40°K. Thus, the error due to this source is less than 0.015 deg at 10°K and less than 0.005 deg at 40°K.

In the case of gold, another difficulty was encountered. Since one wishes to obtain 0.01 deg temperature accuracy, it is imperative that the temperature difference between the center and ends of the specimen due to the heat conduction from the thermocouple lead wires be

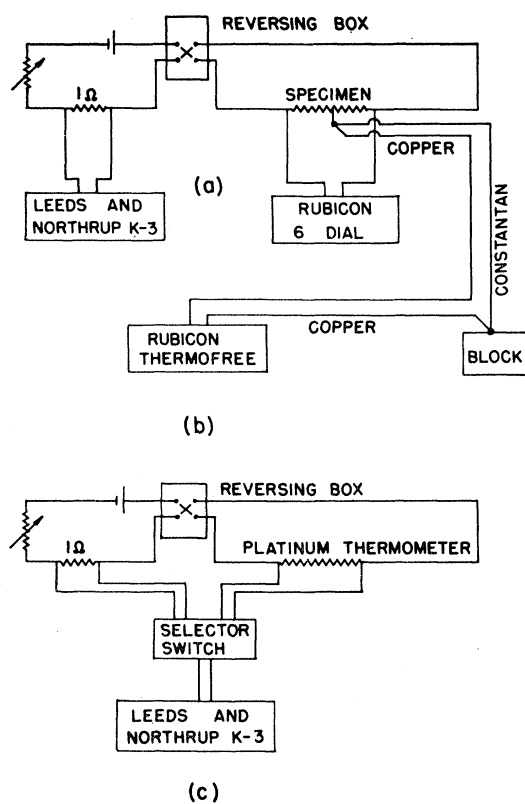


FIG. 2. Electrical and temperature measurement circuits.

less than 0.01 deg. An estimate of this effect can be made as follows. Let  $T_0$  be the temperature at the ends of the specimen,  $T_1$  be the temperature of the thermocouple lead wires where they last touch the block,  $T_m$  be the temperature of the middle of the specimen,  $k$  be the thermal conductivity,  $l$  be the length of the conduction path,  $A$  be the cross-sectional area of the conductor, the subscript  $s$  refer to the specimen, the subscript  $L$  refer to the leads. One then finds that in the steady-state condition

$$T_m - T_0 = (T_1 - T_0) \left[ 1 + \left( 2 \frac{k_s A_s}{l_s} / \frac{k_L A_L}{l_L} \right) \right]^{-1}.$$

Now for gold,  $k = 10$  W/cm deg,  $A_s = 19 \times 10^{-6}$  cm<sup>2</sup>,  $l_s = 0.5$  cm. Therefore,

$$k_s A_s / l_s = (19 \times 10^{-5}) / (5 \times 10^{-1}) = 3.8 \times 10^{-4} \text{ W/}^\circ\text{K}.$$

Assuming  $T_1 - T_0 = 1$  deg, we find that for  $T_m - T_0 \leq 0.01$  deg we must have  $k_L A_L / l_L < 8 \times 10^{-6}$  W/deg. The conductivity of copper at low temperature is approximately 10 W/cm deg. Therefore,  $A/l < 8 \times 10^{-7}$ . Thus, we find  $d^2(\text{mils})/l(\text{cm}) < 10^{-1}$ . We would require a length of 160 cm of 4-mil-diam wire. This is obviously not feasible. Therefore, a 40-cm length of 2-mil copper wire was used from the last contact with the block to the specimen.

With these two precautions, one is able to measure the temperature to 0.1 deg below 10°K, 0.04 deg be-

tween 10 and 15°K, 0.03 deg between 15 and 20°K, 0.01 deg between 20 and 25°K, and to better than 0.01 deg above 25°K. The temperature control is actually much better than this as will be explained under Data.

### Measurement of Resistance

The resistance measurements were made in the usual manner by a direct application of Ohm's law with the potential across the specimen measured with a Rubicon 6-Dial Potentiometer with a photoelectric galvanometer and the current measured by means of the voltage produced across a 1-ohm standard resistor. This voltage was measured by a Leeds and Northrup K3 potentiometer. The current was controlled by means of a variable resistor in series with the specimen. In order to eliminate parasitic emf's readings were taken in pairs with current flowing in opposite directions. The two specimens were entirely independent, i.e., separate potentiometers and current systems for each. A schematic drawing of the circuitry is shown in Fig. 2(a).

The voltage measurements have an absolute accuracy of 1 in  $10^4$ . The finest control on the current was 1 in  $6 \times 10^3$  so that the maximum swing either way was 1 in  $12 \times 10^3$ . Therefore,  $\Delta R/R \leq 2 \times 10^{-4}$ .

### Irradiation Procedure

The irradiation was performed on the Northwestern University Van de Graaff. After passing through the bending magnet and its accompanying 1-cm  $\times$  1-cm aperture, the beam passed down an 8-ft length of 2 1/4-in.-diam aluminum pipe. The divergence of the beam was such that it filled the pipe approximately 4 ft from the magnet. At that point a 1/2-mil aluminum foil was inserted to separate the Van de Graaff from the cryostat vacuum system and thus prevent contamination of the low-temperature parts by deposition of mercury vapor. A water-cooled 9/16-in.  $\times$  15/16-in. aperture was placed 6 in. from the specimen. The final, and essentially only defining of the beam was done by a 1/8-in. thick copper aperture on the front of the liquid nitrogen shield. This aperture was identical in shape and about 1/32-in. smaller than the corresponding opening in the mounting block [Fig. 1(b)]. Thus the beam passed through a foil 4 ft from the bending magnet and entered the defining aperture 1 in. from the specimens. The entire system was aligned optically and the alignment checked by a phosphor-coated plate placed behind the specimen. A further check on the alignment was provided by the fact that the helium loss rate remained low during irradiation.

The beam was terminated by a Faraday cage placed behind the specimens such that all electrons passing through the defining aperture entered the cage. The cryostat was grounded and electrically insulated from the Faraday cage. The charge collected was passed through a current integrator to ground. The current

density was obtained by dividing the current by the area of the defining aperture.

During irradiation, the maximum temperature of the gold specimen was 8.5°K and the cadmium specimen was 8°K. It was found that initially current densities of approximately  $0.22 \times 10^{-6}$  A/cm<sup>2</sup> could be used, but that this value had to be steadily reduced to a final value of  $0.15 \times 10^{-6}$  A/cm<sup>2</sup>. The temperature of the specimens during irradiation was continuously measured as described above. Since the thermocouple readings for gold tended to increase for the same bombarding current, the authors feel that the thermal conductivity of gold was lowered due to the irradiation damage. It was necessary to "hold" at 6°K for a total of 11 days due to difficulties with the Van de Graaff. During this time no annealing of the accumulated damage was observed.

Damage production as a function of flux showed some interesting features. The curves for both cadmium and gold are linear except for discontinuities at several points (see Fig. 3). One notes that the gold curve consists of four parallel segments and the cadmium curve of two. Therefore, whatever process is occurring is not associated with the system as a whole, but rather with an individual specimen. No temperature fluctuations were observed in the thermocouples; however, it must be remembered that only one was being continuously recorded at a time, and thus a complete record is not available.

The total flux obtained was  $7.5 \times 10^{17}$  electrons/cm<sup>2</sup>. The energy of the beam was  $3.0 \pm 0.1$  MeV. The energy loss through the  $\frac{1}{2}$ -mil aluminum foil was negligible. The maximum energy loss in the gold specimen is 0.2 MeV and the average loss 0.13 MeV. In the cadmium specimen, the energy loss is 0.09 MeV. The total damage put in was  $8.46 \times 10^{-9}$  Ω-cm in gold and  $2.32 \times 10^{-9}$  Ω-cm in cadmium. To compute the damage per electron/cm<sup>2</sup>, one must use the slopes of the straight segments in the damage production curves and divide by the area of

$1.21$  cm<sup>2</sup>. When this is done, one obtains the values  $1.2 \times 10^{-26}$  Ω-cm/(electron/cm<sup>2</sup>) for gold and  $4.29 \times 10^{-27}$  Ω-cm/(electron/cm<sup>2</sup>) for cadmium.

### III. DATA

The annealing datum obtained in this experiment is the resistance as a function of time for a series of temperatures. The data-taking procedure was as follows. At time  $t=0$ , a timer is started and a boosting current is supplied to the heater windings to raise the temperature. When the desired temperature is reached, usually after 1 min, the time is recorded and resistance readings commence. For each specimen the voltage and time are recorded simultaneously, the direction of the current is reversed between readings. This procedure is carried on continuously as long as appreciable changes in resistance are occurring. Concurrently with this, thermocouple readings are taken at frequent intervals. The temperature is maintained for 60 min at which point the identical process is started at the next higher temperature.

This procedure was carried out in  $1\frac{1}{2}$  deg steps to 21°K, in 2 deg steps from 23 to 45°K, in 3 deg steps from 48 to 51°K and 4 deg steps from 55 to 67°K. In addition the specimen was cooled to the lowest temperature available (6°K) and resistance measurements made after anneals at 18, 27, 35, 43, and 51°K. After such a measurement the system was heated to a temperature a degree below that of the last anneal and stabilized. The timer and booster current were then started and the process continued as discussed above.

The data thus obtained are reduced in the following way. The voltage readings are plotted as a function of time on the same plot for both directions of the current. A curve is then drawn through each set of points, and from these two curves an average curve can be constructed with the parasitic emf's eliminated. This was done for each specimen at each temperature. If the temperature coefficient of resistance were low this would be the desired plot. However, in the cases of gold and cadmium the coefficients are both approximately 1200  $\mu\Omega/^{\circ}\text{K}$  near 25°K. In gold 15  $\mu\Omega$  anneal typically in 60 min. Thus it is clear that temperature control of 0.01°K would produce a large background masking the effect. Two fortunate facts help in this regard. Although the absolute temperature is known to only  $\pm 0.01^{\circ}\text{K}$ , the actual temperature fluctuations are only 0.005°K and are of short duration. Secondly, very little annealing occurs in cadmium; thus it is possible to use it as an additional thermometer. One merely selects the average value of the voltage for cadmium during a specific anneal, measures the deviation from that voltage at a given time, converts that deviation into a temperature difference, and converts the temperature difference into a voltage deviation on the gold curve. In this manner, one is able to considerably reduce the fluctuation. The curves thus obtained are shown in Fig. 4 up to 35.18°K for gold.

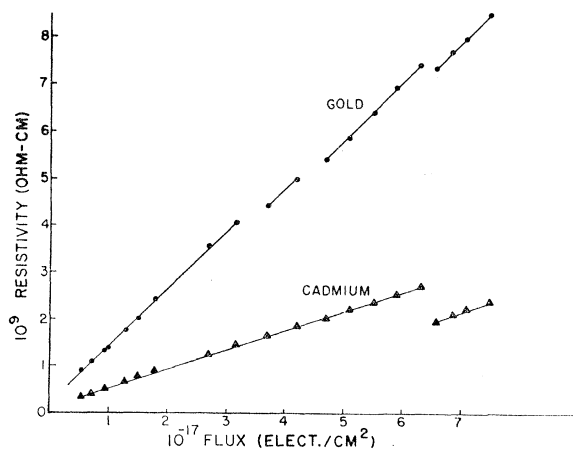


FIG. 3. Damage production as a function of flux for gold and cadmium.

A valuable check on the accuracy of the method is obtained from the low-temperature measurements made at 18, 27, 35, 43, and 51°K by noting that the amount annealed between two of these readings must equal the sum of the amounts in each anneal as obtained from the difference in end points of the voltage vs time curve for an anneal. These values agree to within 9, 18, 7, 12, and 30% for the intervals ending at 18, 27, 35, 43, and 51°K, respectively.

Unfortunately, the above method cannot be applied to cadmium. Also, since the amount annealing out is very small, the scatter completely masks the effect and nothing can be obtained from the annealing curves. However, one does obtain the amount annealed between successive low-temperature measurements. These results are shown in Fig. 7.

Before the irradiation the resistance vs temperature curve for each specimen was obtained. A comparison of these curves with the values of the resistance at the starting point of each anneal enables one to determine the deviations from Matthiessen's rule, as discussed under Calculations.

#### IV. CALCULATIONS

##### Activation Energy Spectrum

One now wants to find the original activation energy spectrum of the annealing processes occurring in gold from the isothermal plots which describe the rate of change of resistance with respect to time for a series of temperatures. It is assumed that the value of a macroscopic quantity, such as the resistance, depends directly on the concentration of defects (in this experiment vacancies and interstitials) in the lattice produced by the electron bombardment. As the temperature of the lattice is raised, during the anneal, lattice vibrations impart enough energy to the defects to enable them to rearrange themselves. Let an activation energy  $E$  be associated with the annealing of each different defect configuration; then, in the following analysis  $R(E)dE$  is

defined to be the amount of resistance which anneals with activation energy in the range between  $E$  and  $E+dE$ . Following Primak,<sup>6</sup> the time rate of change of  $R(E)$  is

$$dR(E)/dt = -R(E)\nu \exp(-E/\tau), \quad (1)$$

where  $\nu$  is a constant having units of frequency.  $\tau = kT$ , product of Boltzmann's constant and the temperature.

It is assumed, in this equation, that the annealing of the close interstitial vacancy pairs of defects is correlated, i.e., first order. However, one expects as the temperature of the lattice is raised that free migration of the defects to fixed sinks will occur (second or higher order). Following Primak,<sup>6</sup> this analysis is, however, a good first approximation to higher orders. The solution to Eq. (1) is

$$R(E) = R_0(E) \exp[-\nu t \exp(-E/\tau)] \equiv R_0(E)\Theta(t, \tau), \quad (2)$$

where  $R_0(E)$  is the original activation energy spectrum before any annealing has occurred.  $\Theta(E, t, \tau)$  as defined by Eq. (2) measures the amount of the original distribution swept out as the annealing time  $t$  increases.  $\Theta$  varies from 0 to 1 over only a small range of  $E$ , being zero for small values of  $E$  and 1 for large values of  $E$ .

Now consider a succession of isothermal anneals in steps of  $\Delta T \approx 0.1T$ . At any one temperature  $T_i$  the function  $\Theta$  sweeps out no longer the original distribution but the original distribution as modified by the successive previous anneals. Then one can write for any one anneal at  $\tau_i = kT_i$ ,

$$R_i(E) = R_{i-1}(E)\Theta(t_i, \tau_i) \equiv R_{i-1}(E)\Theta_i, \quad (3)$$

where  $t_i$  is the time as measured from the beginning of the  $i$ th anneal, as discussed under Data. Carrying through the successive substitutions, one has for the  $n$ th anneal

$$R_n(E) = R_0(E) \left[ \prod_{i=1}^{n-1} \Theta_i \right] \Theta_n. \quad (4)$$

The quantity that is experimentally measured during the  $n$ th anneal is the total resistance  $R_n^{\text{tot}}$ , where

$$R_n^{\text{tot}} = \int_0^\infty R_n(E) dE. \quad (4)$$

Then for any two points  $(R_1, t_1)$ ,  $(R_2, t_2)$  on the same isothermal curve, characterized by  $\tau$ , the total resistance change occurring after  $n-1$  previous anneals is

$$R_1^{\text{tot}} - R_2^{\text{tot}} = \int_0^\infty [R_1(E) - R_2(E)] dE. \quad (6)$$

Substituting in the integrand the appropriate expression

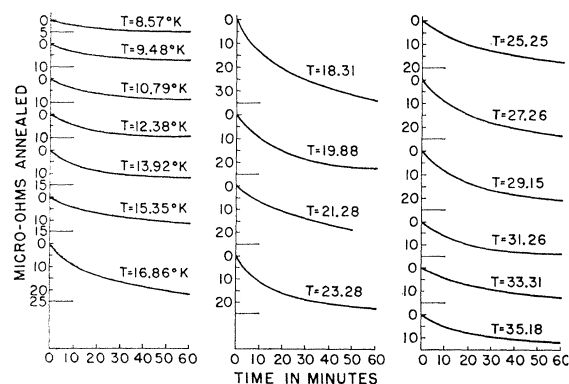


FIG. 4. Isothermal annealing data for gold from 8.57 to 35.18°K. (The abnormal time, i.e., less than 60 min, of the 21.2°K plot was due to an experimental difficulty.)

<sup>6</sup> W. Primak, J. Appl. Phys. 31, 1524 (1960).

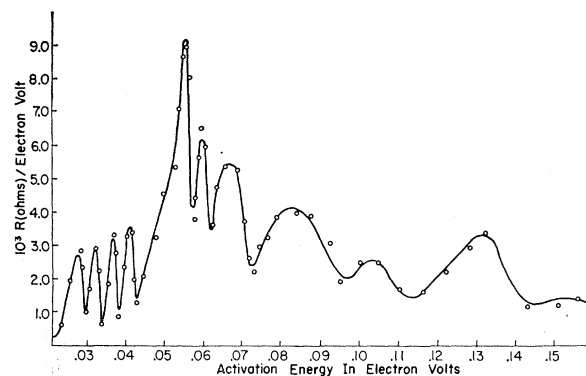


FIG. 5. Activation energy spectrum for gold.

for  $R_1(E)$  and  $R_2(E)$  from Eq. (4) one gets

$$R_1^{\text{tot}} - R_2^{\text{tot}} = \int_0^\infty R_0(E) \left[ \prod_{i=1}^{n-1} \Theta_i \right] \times [\Theta(E, t_1, \tau) - \Theta(E, t_2, \tau)] dE. \quad (7)$$

The second bracketed term in the integrand has an appreciable value only for a small range of  $E$  since it represents the difference between two functions of the same shape, slightly displaced from each other along the  $E$  axis, and both varying from zero to one over a small range of  $E$ . If one assumes that  $R_0(E)$  is sufficiently broad over this range of  $E$ , one can for the zeroth approximation assume  $R_0(E)$  constant and equal to  $R_{00}(\bar{E})$ .  $\bar{E}$  is a suitable average activation energy over the interval of integration for which the integrand does not vanish. Let

$$A_{12} = \left[ \prod_{i=1}^{n-1} \Theta_i \right] [\Theta(E, t_1, \tau) - \Theta(E, t_2, \tau)].$$

Substituting in Eq. (7) for  $R_0(E)$  the constant  $R_{00}(\bar{E})$  and  $A_{12}$  one gets

$$R_{00}(\bar{E}) = (R_1^{\text{tot}} - R_2^{\text{tot}}) / \int_0^\infty A_{12} dE, \quad (8)$$

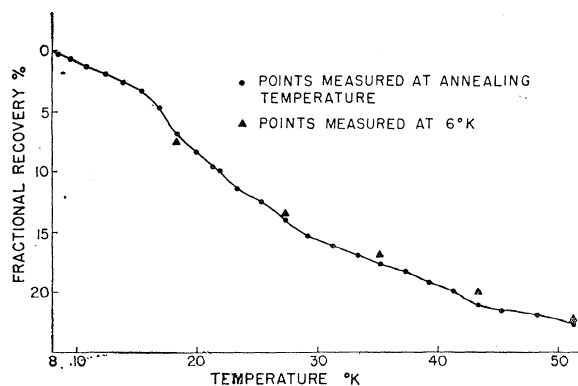


FIG. 6. Isochronal fractional recovery plot for gold.

where the definition of  $\bar{E}$  is

$$\bar{E} = \int_0^\infty E A_{12} dE / \int_0^\infty A_{12} dE. \quad (9)$$

Figure 5 is a plot of  $R_{00}(\bar{E})$  vs  $\bar{E}$ . The points for this plot were computed in the following manner. From each isothermal curve the values of  $R_1^{\text{tot}} - R_2^{\text{tot}}$ ,  $t_1$ , and  $t_2$  were recorded for approximately 8 intervals. Then the value of the integrals appearing in Eqs. (8) and (9) were calculated on a computer for each interval. The authors are indebted to Dr. K. Herschbach for the program used for these calculations. Only representative points are shown in Fig. 5; considerably more points were used to determine the final curve of the initial activation energy spectrum.

A determination of the frequency factor from the initial activation energy spectrum, as described by Primak, was attempted. Plots of the initial activation energy spectrum were made for values of  $\nu = 7.2 \times 10^{10}$

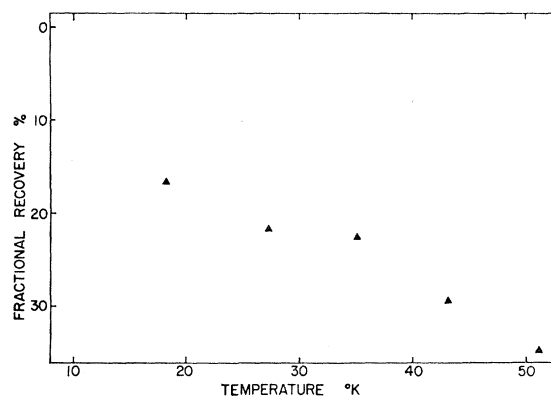


FIG. 7. Isochronal fractional recovery plot for cadmium.

$\text{sec}^{-1}$ ,  $\nu = 5.3 \times 10^{11} \text{ sec}^{-1}$ ,  $\nu = 3.9 \times 10^{12} \text{ sec}^{-1}$ . It was found that the segments of the curve joined more smoothly with  $\nu = 5.3 \times 10^{11} \text{ sec}^{-1}$  than in the other cases. However, the uncertainty in the data was too large for a determination of  $\nu$  to the accuracy that this method usually offers. A frequency factor  $\nu = 5.3 \times 10^{11} \text{ sec}^{-1}$  was used for the activation energy plot shown in Fig. 5.

The isochronal plot for gold, Fig. 6, was obtained by measuring the amount of resistivity annealed out at each annealing temperature as found from the isothermal plot. The percent fractional recovery is based on the resistivity change induced by the damage. The resistivity recovery as measured at 6°K is indicated by separate points. As discussed above, the only meaningful recovery data for cadmium were those obtained at 6°K after each temperature increase of 9°K, Fig. 7.

Since the isothermal annealing steps taken were 2 and 3°K above 21 and 45°K, respectively, the resolution of the peaks in the plot of the slope of the isochronal recovery, Fig. 8, is limited. The authors merely consider

this plot to be a supplementary result. The prime experimental result is the activation energy plot as obtained from the isothermal annealing.

A discussion of the reliability of the first four small peaks of the activation energy plot is in order. In this temperature range small changes in the shape of the isothermal curve have a large effect on the activation energy since the total amount annealing in any one step is small. Thus, it is possible to combine two of the small peaks into one second-order peak. However, this would require a change of the excellent agreement in the amount that annealed out up to 18°K as measured at the annealing temperatures and at 6°K, respectively. It is also felt that a second-order process is highly unlikely at such a low activation energy. The position of the peaks relative to each other in this range is certain to within  $\pm 0.002$  eV for the particular frequency factor chosen.

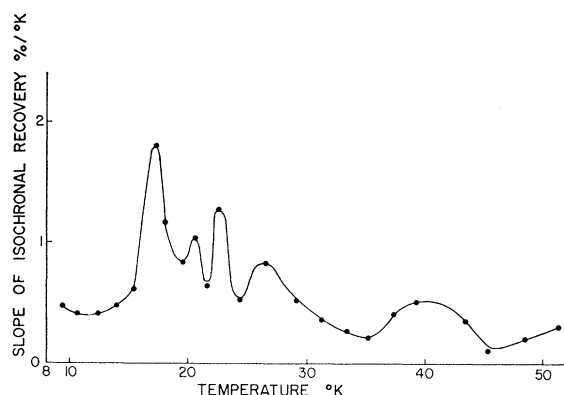


FIG. 8. Plot of the slope of isochronal recovery of gold.

### Deviation from Matthiessen's Rule

Kohler<sup>7</sup> pointed out that, due to the interaction of the lattice vibrations and defects in the lattice, a deviation  $\Delta(T)$  exists in Matthiessen's rule:

$$\rho(T) = \rho_T(T) + \rho_R + \Delta(T),$$

where  $\rho_T$  = resistivity due to lattice vibrations, and  $\rho_R$  = residual resistivity due to defects. Sondheimer<sup>8</sup> calculated the deviation for monovalent metals. An example of his results and calculation for multivalent metals are given in an article by Krantz and Schultz.<sup>9</sup> For this experiment  $\Delta(T)$  is actually the difference in deviations from Matthiessen's rule of the metals before and after irradiation:

$$\Delta(T) = \rho'(T) - \rho(T) - \rho_D(T),$$

where  $\rho'(T)$  is the resistance after irradiation,  $\rho(T)$  is the resistance before irradiation,  $\rho_D$  = resistance due

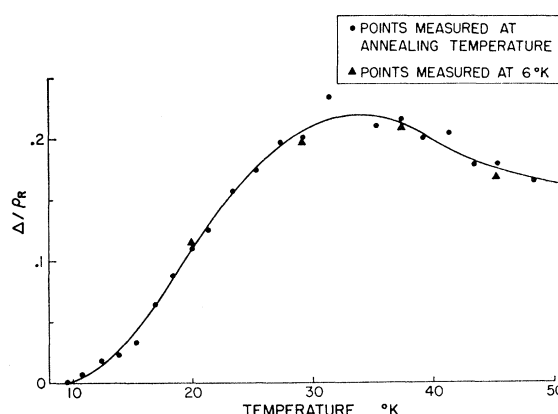


FIG. 9. Deviation from Matthiessen's rule for gold.

to defects which have not annealed out up to temperature  $T$ .

The shape of the plot of  $\Delta(T)/\rho_R$  against  $T$  for gold and cadmium is in good agreement with the experimental results given in reference 3.  $\rho_T = \rho_R$  at 19°K where  $\rho_R$  is the residual resistance. The magnitude of  $\Delta(T)/\rho_R$  is larger than one would expect for the concentration of defects. Figure 9 is the plot for gold and Fig. 10 is the plot for cadmium.

## V. DISCUSSION OF RESULTS

### Cadmium

The interpretation of the cadmium results obtained in this experiment is necessarily rather vague. One can say that, as in the case of gold, a relatively small amount of the damage put in at 8°K anneals out in the range from 8 to 67°K. (Note that the annealing was carried out to 67°K although detailed analysis was applied only to the data up to 51°K.) While the data from this experiment were being analyzed, Coltman *et al.*<sup>10</sup> of Oak Ridge reported on an irradiation and isochronal anneal performed on cadmium making use of the high cross section (2550 b) for the  $(n, \gamma)$  reaction with thermal

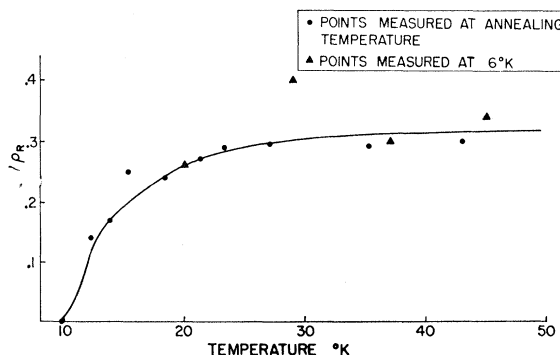


FIG. 10. Deviation from Matthiessen's rule for cadmium.

<sup>7</sup> M. Kohler, Z. Physik **126**, 495 (1949).

<sup>8</sup> E. H. Sondheimer, Proc. Roy. Soc. (London) **A203**, 57 (1950).

<sup>9</sup> E. Krantz and H. Schultz, Z. Naturforsch **12A**, 710 (1957).

<sup>10</sup> C. E. Klabunde, R. R. Coltman, and D. L. McDonald, Bull. Am. Phys. Soc. **7**, 172 (1962).

TABLE I. Summary of the results obtained in three annealing experiments on gold.

	(a)	(b)	(c)
Energy and type of bombarding particle	21-MeV deuterons	3-MeV electrons	2.5-MeV electrons
Total flux, particles/cm <sup>2</sup>	$2.5 \times 10^{16}$	$7.5 \times 10^{17}$	$2 \times 10^{16}$
Resistivity increase (ohm-cm)	$4.5 \times 10^{-8}$	$8.5 \times 10^{-9}$	$3.5 \times 10^{-10}$
ohm-cm/(particle/cm <sup>2</sup> )	$170 \times 10^{-26}$	$1.2 \times 10^{-26}$	$1.6 \times 10^{-26}$
Residual resistivity	$2.7 \times 10^{-9}$ at 6°K	$3 \times 10^{-9}$ at 6.3°K	$1.9 \times 10^{-9}$ at 8°K
Recovery of damage			
10 -16.5°K	4.4%	4.7%	6.9%
16.5-20.5°K	3.0%	4.3%	9.0%
20.5-25°K	1.6%	3.3%	5.0%
25 -38°K	5.5%	6.3%	8.0%
38 -51°K	2.8%	3.9%	4.8%
Total 10-51°K	17.3%	22.5%	33.7%

<sup>a</sup> See reference 2.<sup>b</sup> Present paper.<sup>c</sup> See reference 3.

neutrons. They observe a large annealing peak at 7°K and considerable annealing below 7°K. This partially explains the low damage production rate observed in the present experiment. The general structure of the low-temperature annealing observed in this experiment, Fig. 7, is in agreement with that obtained by Coltman although the amount of annealing is somewhat less.

### Gold

A discussion of the results of gold should have as its starting point a comparison with the corresponding results of the other two noble metals, copper and silver. It has been well established that the low-temperature annealing spectrum of these metals consists of three rather narrow, concentration-independent peaks, a broad, concentration-independent peak containing approximately 48% of the total annealing of 1.4-MeV electron produced damage, and a small broad concentration-dependent peak.<sup>11</sup> In copper the fourth ( $I_D$ ) peak is at about 0.11 eV, in silver, at 0.08 eV.<sup>5</sup> The relative size of the peaks and the total amount of anneal-

ing below 60°K depend somewhat on the bombarding particle. In the case of 1.4-MeV electrons 74% of the damage in copper anneals in the first four peaks.<sup>11</sup> With 10-MeV deuteron bombardment, 57% of the damage in copper and 37% in silver, anneal in the first four peaks.<sup>5</sup>

To date there have been three detailed annealing experiments on gold: Ward and Kauffman<sup>3</sup> using 2.5-MeV electrons, Herschbach<sup>2</sup> using 21-MeV deuterons, and the one described in this paper. A summary of the results from 12°K, or 0.037 eV on, is given in Tables I and II. From these tables, one can note that the results of the present experiment are in good agreement with those of Ward and Kauffman.<sup>3</sup>

If one compares the experimental results of copper and silver as summarized above and the results for gold as given in Tables I and II, one notes that there is a fundamental difference in the annealing spectrum of gold and that of copper and silver. There are a greater number of first-order peaks in gold and the total amount of annealing up to 51°K in gold is substantially less than that of copper. A possible explanation for the small amount of low-temperature annealing is to be found in

TABLE II. Location of the annealing peaks observed in three annealing experiments on gold. Activation energy calculated from a frequency factor =  $5 \times 10^{11}$  sec<sup>-1</sup>.

Peak	(a)		Position		(c)		Recovery		
	(°K)	(eV)	(b) (eV)	(°K)	(eV)	(a) (%)	(b) (%)	(c) (%)	
1	12.1		0.037			1.6	0.6		
2	14.5		0.041	14.5	0.044	1.4	1.0	6.1	
3	18.3		0.055	18.3	0.053	2.4	2.9	7.9	
4			0.059				1.7		
5			0.066	22.5	0.067		3.1	4.4	
6	28.5		0.083	28	0.083	1.4	4.7	7.1	
7	33.5	0.103	0.103			3	1.7		
8	44	0.140	0.131	42	0.123	1.8	3.6	3.9	

<sup>a</sup> K. Herschbach, Phys. Rev. (to be published).<sup>b</sup> Present paper.<sup>c</sup> J. B. Ward and J. W. Kauffman, Phys. Rev. 123, 90 (1961).

<sup>11</sup> J. W. Corbett, R. B. Smith, and R. M. Walker, Phys. Rev. 114, 1460 (1959).



the focusing collisions first suggested by Silsbee,<sup>12</sup> and strong interstitial clustering as suggested by Ward and Kauffman.<sup>3</sup>

The fact that the annealing spectrum is qualitatively different in gold than in copper and silver is of great importance since any scheme of imperfections used for interpretation must enable one to understand the fact that the noble metals can behave so differently. Leibfried suggested that the interstitial configuration may be different in gold from its configuration in copper and silver. This possibility will be examined in a later paper.

## VI. CONCLUSION

The low-temperature annealing spectrum of gold consists of at least 9 peaks ranging in activation energy from 0.02 to 0.15 eV for a frequency factor of  $5.3 \times 10^{11}$  sec<sup>-1</sup>. The total percentage of the original damage annealed out up to 51°K is 22.5%. The annealing be-

havior of cadmium is in qualitative agreement with earlier measurements.

The following conclusions can be made: (1) The amount of close pair recovery in gold is substantially smaller than in copper; (2) the close pair recovery spectrum in gold is more complex than that of copper. In the three experiments done on gold it is not possible to locate an annealing peak which is dose-dependent. It would be valuable to do careful isochronal annealing experiments aimed at determining whether any of the annealing peaks observed shift in temperature when the amount of damage is altered.

## ACKNOWLEDGMENTS

The authors wish to acknowledge the invaluable assistance rendered by the radiation damage groups of Illinois and Northwestern during the irradiation and the annealing measurements. The authors are indebted to Dr. K. Herschbach for assistance in other parts of this experiment and for the suggestion of the deviation from Matthiessen's rule.

<sup>12</sup> R. H. Silsbee, J. Appl. Phys. **28**, 1246 (1957).

## Longitudinal Nuclear Magnetic Relaxation in Ferromagnetic Iron, Cobalt, and Nickel\*

M. WEGER†

*University of California, Berkeley, California*

(Received July 9, 1962)

The longitudinal nuclear relaxation time  $T_1$  has been measured in ferromagnetic iron, cobalt, and nickel. A model is presented to account for the measured values. In the Bloch walls, the relaxation is due mainly to domain wall fluctuations. In the domains, the relaxation is due to interaction of the conduction electrons with nuclei via spin waves. The expression for  $T_1$  due to this process is  $1/T_1 = (kT/h)(\omega/\omega_d)^2 a^2 \Sigma / (32\pi^3 S^2)$ , where  $\omega$  is the nuclear resonant frequency,  $a$  is the lattice constant,  $\omega_d$  is the parameter describing the spin wave spectrum  $E(k) = \hbar \omega_d a^2 k^2$ ,  $S$  is the average spin per atom, and  $\Sigma$  is the area of the Fermi surface per cubic unit cell. If the experimental value of  $T_1$  is used in this formula to determine  $\Sigma$ , then in cobalt,  $\Sigma$  will agree closely with the area of a spherical surface containing about one electron per atom. In iron and nickel,  $\Sigma$  will be about three times larger.

## INTRODUCTION

**N**UCLEAR magnetic resonance (NMR) in a ferromagnetic metal was first observed by Gossard and Portis<sup>1</sup> in metallic cobalt. These authors investigated the resonance and described its salient features: the resonant frequency and its temperature dependence, the linewidth, the spin-spin and spin-lattice relaxation processes. However, the experimental apparatus employed in these experiments was designed for the interpretation of equilibrium spectra, and the purpose of the work reported in this paper is to study relaxation

processes which can be investigated more directly by use of NMR pulse techniques.<sup>2</sup>

The experiments described in the present paper indicate that the longitudinal relaxation process can be understood in terms of two mechanisms: a nonexponential relaxation observed at low rf power levels which is believed to be due to thermal fluctuations of the domain walls, and an exponential relaxation observed at high rf power levels which is believed to be due to an interaction of the conduction electrons with the nuclei via spin waves. This model is used to determine experimentally the area of the Fermi surface. In cobalt the area determined this way is consistent with a model in

\* Supported by the Office of Naval Research.

† Present address: University of California, La Jolla, California.

<sup>1</sup> C. Gossard and A. M. Portis, Phys. Rev. Letters **3**, 164 (1959); J. Appl. Phys. **31**, 205S (1960).

<sup>2</sup> M. Weger, A. M. Portis, and E. L. Hahn, J. Appl. Phys. **32**, 124S (1961).